Reference 63

Modified Suspended Membrane Photonic Crystal D_3 Laser Cavity With Improved Sidemode Suppression Ratio

Wan Kuang, J. R. Cao, Sang-Jun Choi, *Student Member, IEEE*, John D. O'Brien, *Member, IEEE*, and P. Daniel Dapkus, *Fellow, IEEE*

***Abstract*—We have demonstrated the ability to selectively modify the mode structure of a multimoded photonic crystal laser cavity, based on the detailed knowledge of resonant modes in a suspended membrane D_3 microcavity. We have designed a microcavity in which the margins between the highest Q mode and the next highest Q modes have been increased. This modified cavity has been shown to have an improved sidemode suppression ratio under high power pumping condition.**

***Index Terms*—Photonic crystal, semiconductor cavity.**

I. Introduction

PHOTONIC crystal laser cavities offer a great deal of freedom to engineer the properties of the lasing mode. As part of the effort to take advantage of this freedom, we believe that it is valuable to demonstrate the ability to experimentally manipulate the localized modes. Instead of constructing localized resonant modes from the photonic crystal band edge modes with relatively weak perturbations [1]–[5], we study the possibility of selecting a candidate mode from a pool of local resonances in a multimode cavity and then selectively improving the modal properties through modifying the multimode cavity geometry. Specifically, we show that a laser cavity can be modified in a way in which the lasing mode is nearly unaffected while the nearby modes have reduced intensity. By introducing six small holes at the nodes of a high quality factor mode in a triangular lattice D_3 membrane laser cavity [6], [7], we were able to suppress the nearby resonant modes within ~50 nm of the lasing mode without perturbing the lasing mode itself.

II. Analysis and Characterization

The photonic crystal defect microcavities were fabricated [8] on an metal–organic chemical vapor deposition grown epitaxial structure consisting of a 60-nm-thick InP layer and 224 nm of InGaAsP layer containing four compressively strained InGaAsP quantum wells designed to emit at 1.5 μm at room temperature. A compound dry etching mask of a 100-nm-thick SiN_x and a 45-nm-thick Au layer was deposited, followed by a 100-nm-thick spin-coated 2% diluted polymethylmethacrylate as an electron beam resist. After the electron beam lithography, 170 s of Ar^+ ion beam milling transferred the pattern into the Au layer. The pattern was further transferred to the SiN_x layer by a CF_4 reactive ion etch. The photonic crystal cavity was finally formed by a CH_4–H_2–Ar electron cyclotron resonance etch followed by a few minutes of HCl: H_2O (4 : 1) wet etch at 0 °C. We have reported previously [6], [7] that such a suspended membrane D_3 photonic crystal cavity, formed by removing three concentric circles of air holes from the triangular photonic crystal lattice, as the one shown in Fig. 1(a) left, supports one dominant high quality factor (Q) mode. A three-dimensional (3-D) finite-difference time-domain (FDTD) simulation of the structure [7] indicates a cold cavity Q over 10 000 for the lasing resonance. The calculation also indicates that more than 95% of the in-plane energy density overlaps with the gain medium and the rest with air holes. Because of the high quality and in-plane confinement factors, this D_3 cavity has a low lasing threshold. Under 8-ns pulsewidth, 1% duty cycle, room temperature optical pumping conditions, incident threshold pumping power as low as 0.5 mW was achieved with this cavity. This incident power level corresponds to about 0.15 mW of absorbed pumping power at threshold considering the finite absorption of the 224-nm InGaAsP membrane and the reflection at the interface between semiconductor and air. Additionally, resonances within ~50 nm of this lasing mode have quality factors that are lowered by nearly an order of magnitude than that of the lasing mode. Experimentally, we observed no mode-hopping above threshold.

The top of Fig. 1(c) also shows the lasing spectrum of one such D_3 laser, when it was optically pumped at about three times threshold. The surface emission from the microcavity is collected vertically from a lens system with a numerical aperture of 0.5 about the normal out-of-plane radiation direction. The calculated resonant frequencies and quality factors for the D_3 cavity are shown in Fig. 1 as gray bars. The calculated resonance wavelengths differ slightly by 25 nm, or 2% from the observed resonance, using averaged dimensions measured from scanning electron microscope (SEM) images of the cavities. The spectral shift between the data and the model is consistent with the fabricated structures having a hole radius that was 15 nm smaller, on average, than the model. Although this cavity has a stable lasing performance, the lower Q resonances within ~50 nm of

Manuscript received October 25, 2004; revised December 23, 2004. This work is based on research supported in part by U.S. Army Research Laboratory and the Army Research Office under contract DAAD19-99-1-0121. Computation for the work described in this letter is supported, in part, by the University of Southern California Center for High Performance Computing and Communications.

The authors are with the Electrical Engineering—Electrophysics Department, University of Southern California, Los Angeles, CA 90089 USA (e-mail: wkuang@usc.edu).

Digital Object Identifier 10.1109/LPT.2005.846761

Report Documentation Page

Form Approved
OMB No. 0704-0188

1. REPORT DATE	2. REPORT TYPE	3. DATES COVERED
01 JUN 2005	**N/A**	**-**

4. TITLE AND SUBTITLE	5a. CONTRACT NUMBER
Modified Suspended Membrane Photonic Crystal D3 Laser Cavity With Improved Sidemode Suppression Ratio	5b. GRANT NUMBER
	5c. PROGRAM ELEMENT NUMBER
6. AUTHOR(S)	5d. PROJECT NUMBER
	5e. TASK NUMBER
	5f. WORK UNIT NUMBER
7. PERFORMING ORGANIZATION NAME(S) AND ADDRESS(ES) **Electrical EngineeringElectrophysics Department, University of Southern California, Los Angeles, CA 90089 USA**	8. PERFORMING ORGANIZATION REPORT NUMBER
9. SPONSORING/MONITORING AGENCY NAME(S) AND ADDRESS(ES)	10. SPONSOR/MONITOR'S ACRONYM(S)
	11. SPONSOR/MONITOR'S REPORT NUMBER(S)

12. DISTRIBUTION/AVAILABILITY STATEMENT
Approved for public release, distribution unlimited

13. SUPPLEMENTARY NOTES
See also ADM001923.

14. ABSTRACT

15. SUBJECT TERMS

16. SECURITY CLASSIFICATION OF:			17. LIMITATION OF ABSTRACT	18. NUMBER OF PAGES	19a. NAME OF RESPONSIBLE PERSON
a. REPORT	b. ABSTRACT	c. THIS PAGE			
unclassified	**unclassified**	**unclassified**	**UU**	**3**	

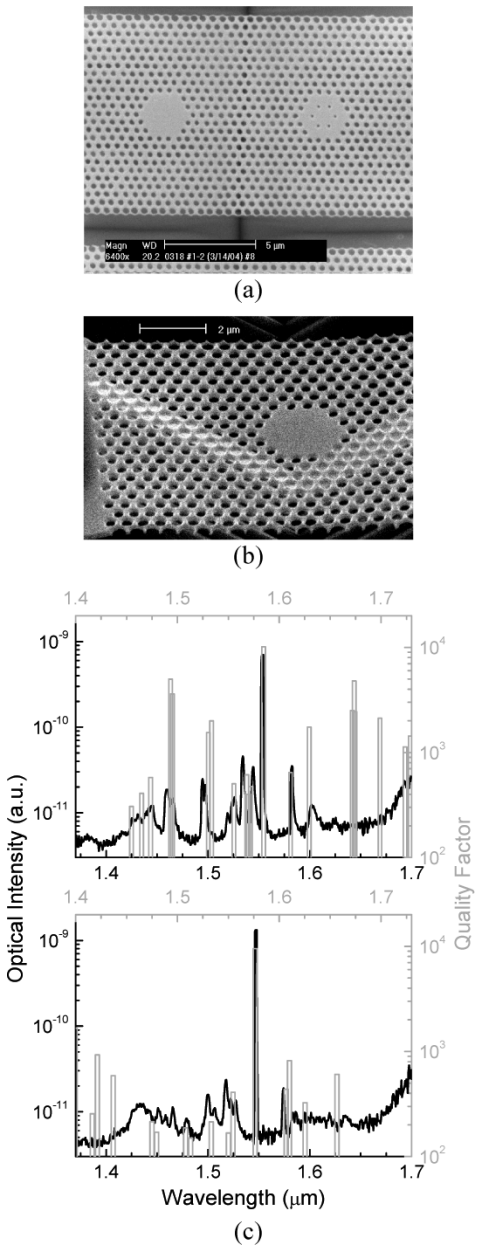

Fig. 1. SEM images showing (a) a pair of suspended membrane photonic crystal D_3 cavities before (left) and after (right) the modification and (b) angle view of a typical suspended membrane photonic crystal D_3 cavities. (c) The lasing spectra for the original (top) and modified (bottom) D_3 microcavities at the same pumping condition, shown in black curves, and the calculated resonant frequencies and quality factors as gray bars. The wavelength axes for the measurement curve (bottom) and the calculation (top) are shifted by 25 nm, or 2%, to account for the frequency difference due to the slight dimension variation for the cavity fabricated and modeled.

the lasing mode still lead to a significant amount of radiation. Especially important in this regard is a doubly degenerate low-Q resonance at about 20 nm to the blue side of the lasing mode. This mode contributes significantly to the measured spectrum because its small far field radiation angle can be very efficiently collected by the lens system [7].

We examine the resonant mode distributions to determine a strategy for improving the properties of this laser cavity. The electric and magnetic fields of the nondegenerate lasing mode are calculated at the midplane of the semiconductor membrane. Due to the mirror symmetry of the cavity along the midplane

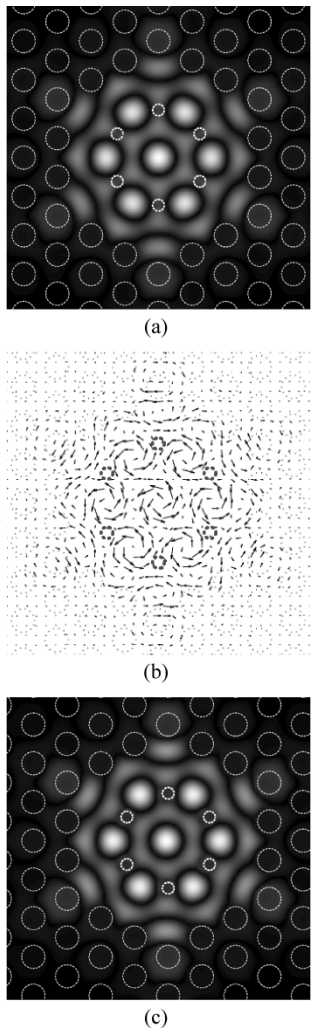

Fig. 2. Intensities of (a) the single vector component magnetic field H_z and (b) vector electric fields E_x and E_y for the nondegenerate lasing mode of a suspended membrane photonic crystal D_3 cavity before modification, in a density plot and vector plot, respectively. (c) The magnetic field H_z for the lasing mode at the midplane of the suspended membrane of the modified D_3 cavity. The dashed gray circles overlaid on both figures show the in-plane dielectric distribution of the microcavity. The six smaller holes drawn in bold indicate the locations for modification, which corresponds to the valleys of the optical intensity of the resonant mode.

of the membrane, the magnetic field at the symmetry plane is a single vector component H_z, where z is the epitaxial growth direction. Simultaneously, the electric field consists of in-plane E_x and E_y components only. Fig. 2 shows the two-dimensional vector electric field and the single vector component magnetic field at the mirror plane in a vector plot and density plot, respectively. There are six valleys of the intensity contour located at roughly 1.2 times the lattice constant a away from the cavity center for both electric and magnetic fields. We, therefore, consider the prospect of improving sidemode suppression ratio of the lasing mode by adding six air holes at the valleys. The resulting change of the permittivity $\varepsilon(\vec{r})$ perturbs both electric field $\vec{E} = \vec{E}_0 + \delta\vec{E}$ and magnetic field $\vec{H} = \vec{H}_0 + \delta\vec{H}$ as

$$\delta\vec{E} = \int d^3r\vec{E}_0(\vec{r}) \cdot \left\{ \frac{1}{\delta\varepsilon(\vec{r})} \nabla \times \left[\nabla \times \vec{E}_0(\vec{r}) \right] \right\} \quad (1)$$

$$\delta\vec{H} = \int d^3r\vec{H}_0(\vec{r}) \cdot \left\{ \nabla \times \left[\frac{1}{\delta\varepsilon(\vec{r})} \nabla \times \vec{H}_0(\vec{r}) \right] \right\} \quad (2)$$

where $\vec{E}_0(\vec{r})$ and $\vec{H}_0(\vec{r})$ are the resonant mode for the original D_3 cavity. The approach to modifying only the nonlasing modes suggested by (1) and (2) is simply to modify the cavity at the intensity minimums of the lasing mode. However, the positions of the intensity valleys for the two fields are slightly displaced by a few percent of a lattice constant. In designing the extra six air holes, we have simply centered them at the half-way point between the electrical and the magnetic field valleys and reduced their normalized radius r/a from 0.3 for the rest of the photonic crystal to 0.15. This simple design is intended to serve as a proof of principle demonstration that the mode structure of a multimoded photonic crystal cavity can be selectively modified.

Given that the field has a relatively small energy distribution at those spatial locations where additional holes were introduced, we expect this modification will preserve the high quality factor and the mode profile of the lasing mode. On the other hand, the nearby resonances do not have nodes at these exact locations. The introduction of these six extra air holes should either increase their scattering loss, which corresponds to the reduction of Qs, or at the very least, it should reduce the in-plane confinement factors relative to the unmodified geometry. We, therefore, expect an improvement in the sidemode suppression ratio.

The prediction is confirmed by the 3-D FDTD simulation of the modified D_3 cavity. The bottom plot of Fig. 1(c) shows the resonant frequencies and the quality factors of the modified D_3 cavity as gray bars. Compared with that of the original structure, the lasing mode has a slightly higher frequency due to a reduced average index. It also experienced a small change in quality factor of less than 10%. Fig. 2(c) shows the magnetic field component H_z for the lasing mode at the midplane of the modified suspended membrane D_3 cavity. Compared with Fig. 2(a), the fields before and after the modification are almost identical except near the six additional holes. It is, therefore, expected that the lasing performance of the cavity is only marginally affected. In contrast, the quality factors for the neighboring resonant modes are decreased by a factor of 3 to 12, as a result of six additional air holes. The contrast has more than tripled the ratio of the Qs between the lasing mode and the next highest resonance in its vicinity.

As a next step, photonic crystal cavities with and without this modification were fabricated experimentally. Details of the fabrication procedure can be found in [6]. Fig. 1(a) shows an SEM image of the modified D_3 cavity along with the original D_3 cavities on the left. To minimize any difference due to fabrication imperfections, these modified and original D_3 cavities were fabricated side by side.

Both cavities were tested under the same pulsed pumping condition. We observed less than a 10% difference in the threshold pumping power of these two devices. The lasing wavelength difference is 6 nm, or less than 5%. This observation is consistent with our previous analysis, which suggests the preservation of the properties of the lasing mode itself. On the other hand, the lasing spectrum under the same pumping condition, i.e., three times the threshold power, of a modified D_3 cavity shows a sidemode suppression ratio that is improved by 7–20 dB compared to the unmodified cavity. In a 50-nm bandwidth around the lasing mode, the fraction of the collected power due to the lasing mode increased from a value of 78% for the original cavity to 92% for the modified cavity. Optical spectra of the original and the modified D_3 cavity are shown as curves in Fig. 1(c) top and bottom, respectively. Both of the spectra are plotted in the same logarithmic scale to facilitate comparison. In addition, most of the resonances on the blue side of the laser line of the modified cavity show a significantly broader line width as a result of predicted lowering of the quality factors of these modes.

III. Summary

We have demonstrated the ability to selectively engineer a particular mode in a multimode photonic crystal microcavity laser through both numerical simulations and experimental characterization. An improved sidemode suppression ratio for the lasing mode is demonstrated on a modified suspended membrane D_3 photonic crystal cavity. The structure is formed by adding six additional reduced-size air holes in the cavity defect where the lasing mode has a small energy distribution.

References

[1] K. Srinivasan and O. Painter, "Momentum space design of high-Q photonic crystal optical cavities," *Opt. Express*, vol. 10, no. 15, pp. 670–687, 2002.

[2] J. Vuckovic, M. Loncar, H. Mabuchi, and A. Scherer, "Optimization of the Q factor in photonic crystal microcavities," *IEEE J. Quantum Electron.*, vol. 38, no. 7, pp. 850–856, Jul. 2002.

[3] K. Srinivasan and O. Painter, "Fourier space design of high-Q cavities in standard and compressed hexagonal lattice photonic crystals," *Opt. Express*, vol. 11, no. 6, pp. 579–593, 2003.

[4] H. Y. Ryu, J. K. Hwang, and Y. H. Lee, "The smallest possible whispering-gallery-like mode in the square lattice photonic-crystal slab single-defect cavity," *IEEE J. Quantum Electron.*, vol. 39, no. 2, pp. 314–322, Feb. 2003.

[5] H. G. Park, J. K. Hwang, J. Huh, H. Y. Ryu, S. H. Kim, and Y. H. Lee, "Characteristics of modified single-defect two-dimensional photonic crystal lasers," *IEEE J. Quantum Electron.*, vol. 38, no. 10, pp. 1353–1365, Oct. 2002.

[6] J. R. Cao, W. Kuang, S. J. Choi, P.-T. Lee, J. D. O'Brien, and P. D. Dapkus, "Threshold dependence on the spectral alignment between the quantum-well gain peak and the cavity resonance in InGaAsP photonic crystal lasers," *Appl. Phys. Lett.*, vol. 83, pp. 4107–9, 2003.

[7] W. Kuang, J. R. Cao, T. Yang, S. J. Choi, P.-T. Lee, J. D. O'Brien, and P. D. Dapkus, "Classification of modes in multimoded photonic crystal microcavities," *J. Opt. Soc. Amer. B*, vol. 22, May 2005, to be published.

[8] J. R. Cao, P.-T. Lee, S.-J. Choi, R. Shafiiha, S.-J. Choi, J. D. O'Brien, and P. D. Dapkus, "Nanofabrication of photonic crystal membrane lasers," *J. Vac. Sci. Technol. B*, vol. 20, no. 2, pp. 618–618, 2002.